



## Open Archive Toulouse Archive Ouverte

OATAO is an open access repository that collects the work of Toulouse researchers and makes it freely available over the web where possible

This is an author's version published in:

<http://oatao.univ-toulouse.fr/27240>

### Official URL

DOI : <https://doi.org/10.1016/j.solidstatesciences.2020.106405>

**To cite this version:** Gibot, P. and Quesnay, F. and Nicollet, C. and Laffont, L. and Schnell, F. and Mory, J. and Spitzer, D. *Detonation synthesis of ZrO<sub>2</sub> by means of an ammonium nitrate-based explosive emulsion*. (2020) Solid State Sciences, 108. 106405. ISSN 12932558

Any correspondence concerning this service should be sent to the repository administrator: [tech-oatao@listes-diff.inp-toulouse.fr](mailto:tech-oatao@listes-diff.inp-toulouse.fr)

# Detonation synthesis of $\text{ZrO}_2$ by means of an ammonium nitrate-based explosive emulsion

P. Gibot<sup>a,\*</sup>, F. Quesnay<sup>b</sup>, C. Nicollet<sup>b</sup>, L. Laffont<sup>c</sup>, F. Schnell<sup>a</sup>, J. Mory<sup>b</sup>, D. Spitzer<sup>a</sup>

<sup>a</sup> Laboratoire Nanomatériaux pour Systèmes Sous Sollicitations Extrêmes (NS3E) UMR 3208 ISL/CNRS/UNISTRA, Institut Franco-allemand de Recherches de Saint-Louis (ISL), 5 Rue Du Général Cassagnou, BP70034, 68301, Saint Louis, France

<sup>b</sup> Laboratoire Physique des Chocs et Détonique, ISL, 5 Rue Du Général Cassagnou, BP70034, 68301, Saint Louis, France

<sup>c</sup> CIRIMAT, Université de Toulouse, CNRS, INP-ENSIACET, 4 Allée Emile Monso, BP 44362, 31030, Toulouse Cedex 4, France

## ARTICLE INFO

### Keywords:

Detonation  
Zirconium (IV) oxide  
Energetic emulsion  
Ammonium nitrate  
Ceramics

## ABSTRACT

A zirconium (IV) oxide powder was successfully synthesized from the detonation of an explosive emulsion previously mixed with zirconium sulfate tetrahydrate salt ( $\text{Zr}(\text{SO}_4)_2 \cdot 4\text{H}_2\text{O}$ ) as a ceramic precursor. After detonation of the energetic mixture in a detonation tank, the as-synthesized ceramic material was purified and characterized by X-ray diffraction, transmission and scanning electron microscopy techniques, nitrogen physisorption and dynamic light scattering. The ceramic powder is made of crystalline nanosized particles exhibiting a homogeneous sphere-like morphology. An attempt to explain the oxide ceramic synthetic mechanism is discussed. The detonation synthetic route implementing high temperatures and high pressures in a short time may be seen as an encouraging method for large-scale production of nanopowder.

## 1. Introduction

Ceramics are of great interest for of scientific research worldwide. Ceramic materials can be of different chemical natures such as oxides ( $\text{Al}_2\text{O}_3$ ,  $\text{TiO}_2$ ,  $\text{ZrO}_2$ ,  $\text{MnFe}_2\text{O}_4$  (ferrite),  $\text{CaTiO}_3$  (perovskite),  $\text{LiMn}_2\text{O}_4$  (spinel)... ) or non-oxides with carbides ( $\text{SiC}$ ,  $\text{TiC}$ ,  $\text{B}_4\text{C}$ ...), nitrides ( $\text{Si}_3\text{N}_4$ ,  $\text{AlN}$ ,  $\text{BN}$ ,  $\text{W}_2\text{N}$ ...) and borides ( $\text{TiB}_2$ ,  $\text{ZrB}_2$ ...) [1]. This diversity in chemical composition explains the numerous and diverse properties exhibited by these materials and consequently the permanent interest in them. For example, ceramics claim high hardness and strength, elevated melting and boiling points, low electrical and thermal conductivities, a chemical inertia and even good optical and magnetic characteristics [1]. Ceramics are therefore a solution of first choice for a plethora of applications in various domains, including catalysis, electronics, magnetism, pyrotechnics, automotive, energy and the environment, aerospace and medical equipment [2].

The physico-chemical properties of ceramics, and from a larger point of view the materials, strongly depend of the synthetic experimental conditions, and authors have suggested and implemented numerous routes or processes to design tailored ceramics (size, morphology, particle-size distribution, aggregation rate, purity...). The synthetic methods include solid thermal decomposition, solid-solid and solid-gas reactions, precipitation, the sol-gel process, the hydrothermal

approach, pyrolysis spray, vapour phase synthesis [3], flame synthesis [4], self-propagating high-temperature synthesis [5], and combustion and detonation routes [6,7]. Regarding this last approach, as per the literature, it can be described as either an instantaneous release of energy at very high temperatures ( $>1000^\circ\text{C}$ ) and pressures ( $>\text{GPa}$ ) over an extremely short time or a chemical decomposition reaction with shock wave generation [8]. From an experimental point of view, these physico-chemical properties seem to be extremely favourable for synthesizing (nano)powders, metastable phases and potentially novel structures. The additional rapid quenching operation at the end of the detonation reaction allows minimization of the growth phenomena. This concept was first used to synthesize nanosized diamond particles from the detonation of a mixture of two organic energetic molecules such as 2, 4,6-trinitrotoluene (TNT) and 1,3,5-trinitro-1,3,5-triazine (RDX) [9]. This result succeeded due to temperatures and pressures as high as 2000–3000  $^\circ\text{C}$  and 20–30 GPa, respectively, corresponding to the diamond stability zone in the carbon phase diagram. This first success encouraged researchers to try producing other inorganic materials and a large majority of oxide materials [7]. For example, diverse oxides were thus synthesized as solid solutions of nanosized cerium oxide-gadolinium oxide ( $\text{Gd}_2\text{O}_3\text{-CeO}_2$ ) [10], manganese ferrite ( $\text{MnFe}_2\text{O}_4$ ) [11], lithium manganese oxide ( $\text{LiMn}_2\text{O}_4$ ) [12], strontium aluminate ( $\text{Sr}_2\text{Al}_2\text{O}_4$ ) [13], titanium oxide ( $\text{TiO}_2$ ) [14], zinc oxide [15]

\* Corresponding author.

E-mail address: [pierre.gibot@isl.eu](mailto:pierre.gibot@isl.eu) (P. Gibot).

zirconium oxide ( $\text{ZrO}_2$ ) [16] or even cerium oxide ( $\text{CeO}_2$ ) [17]. This approach was patented by Innovnano, a manufacturer marketing yttria-stabilized zirconia nanopowder [18–20]. All of these investigations describe the precise control of the morphology, stoichiometry and particle size of the synthesized products depending on the explosive used. Recently, detonation synthesis was successfully used for producing high value carbide ceramics such as silicon carbide nanoparticles ( $\text{SiC}$ ) from a [TNT/RDX-polycarbosilane] composite [21].

Herein, a successful synthesis of zirconium (IV) oxide ceramic particles by means of the detonation of a totally mechanically insensitive zirconium-doped ammonium nitrate-based explosive emulsion is reported. An explosive emulsion, such as Emulstar 3000, and zirconium sulfate hydrate were used as the explosive and ceramic precursor, respectively. In contrast to the literature, where the impact-sensitive RDX secondary explosive is used as the energy source in a non-negligible number of investigations [10,12–14,16], which may contribute to creating a hazardous environment for the operator [22, 23], the Emulstar 3000 explosive emulsion is likely insensitive. More, while zirconium carbonate was used as the Zr-source in Ref. [19], and the Zr-sulfate salt was preferred here due to its high water-solubility, which may lead to a more homogeneous mixture with an explosive emulsion (water/oil mixture). After detonation, the product in the soot was characterized using the usual laboratory techniques.

## 2. Experimental section

Zirconium sulfate tetrahydrate ( $\text{Zr}(\text{SO}_4)_2 \cdot 4\text{H}_2\text{O}$ , 99%) was purchased from Alfa Aesar (Ward Hill, MA, USA). The Emulstar 3000 explosive emulsion was obtained from Titanobel (Pontailler, France). According to the data provided by the manufacturer, the explosive emulsion is composed of ammonium nitrate ( $\text{NH}_4\text{NO}_3$ , 70 wt %), sodium nitrate ( $\text{NaNO}_3$ , 20 wt %) and a mixture of water, oil and surfactant (10 wt %). Some characteristics of the explosive emulsion are given in Table 1. The booster was home-prepared from graphitic carbon and a wax/1,3,5-trinitro-1,3,5-triazinane secondary explosive (RDX,  $\text{C}_3\text{N}_3\text{H}_6(\text{NO}_2)_3$ , Eurochem, Massy, France) mixture. The components were mixed according to a mass ratio of 0.5:5:94.5%. An SA4000 electric initiator from Davey Bickford (Héry, France) was used to ignite the detonation reaction.

### 2.1. Preparation of the explosive emulsion/ceramic salt mixtures

Typically, the zirconium-based explosive mixture was prepared as follows:  $\text{Zr}(\text{SO}_4)_2 \cdot 4\text{H}_2\text{O}$  was added to the commercial explosive emulsion in a 10:90 wt ratio and mixed with a Turbula® mixer (model T2A, W.A. Bachofen) at 23 rpm for 20 min. The mixture (~250 g) was placed in a polypropylene tube ( $\varnothing = 43$  mm,  $L = 150$  mm, Supporting Information) according to a loading density of  $1.15 \text{ g/cm}^3$ . The charge was placed in a plastic bag containing distilled water and hung in the centre of a steel detonation tank. The water medium was used to achieve a high quenching rate of the detonation products. A booster (55 g,  $\varnothing = 28.4$  mm,  $L = 57.5$  mm) and an electric initiator (SA4000, Davey Bickford) were used to complete the energetic train. After the detonation, the soot coated on the inner wall of the tank was collected, filtered to remove plastic and copper fragments and calcinated ( $800^\circ\text{C}$ , 2 h) to remove the carbon phase that may originate from the combustion of the

polypropylene tube.

### 2.2. Characterization techniques

#### 2.2.1. Characterizations of the explosive emulsion/ceramic salt mixture

Before the preparation of large quantities of the explosive emulsion/ceramic salt mixture dedicated to the detonation experiments, small batches (5 g) were prepared and subjected to diverse security tests (shock, friction and thermal stresses) to validate their safe preparation and handling for the operator.

The impact sensitivity threshold, expressed in joules (J), was determined by means of a fall-hammer apparatus. The principle is based on the dropping of weights (1 or 5 kg) from an adjustable height on the sample ( $40 \text{ mm}^3$ ) embedded between two metallic cylinders. The friction sensitivity test was performed on a Julius Peter BAM device (Suceasca 1992). The friction sensitivity, given in newton (N), is measured by scraping the powder ( $10 \text{ mm}^3$ ) between a ceramic stick and a ceramic plate. The force of the stick is determined by the position of weights suspended from the lever bearing the stick. The mechanical sensitivity values (shock and friction) correspond to the value of six consecutive “no-go”, i.e., without any reaction (colour change, combustion reaction, clapping sound...). Regarding the thermal sensitivity of the explosive mixture, differential scanning calorimetric analysis (AQ 20, TA Instrument, New Castle, DE, USA) was implemented. A 1–2 mg sample of mixture was placed in a sealed gold crucible and heated from 25 to  $400^\circ\text{C}$  following a heating rate of  $4^\circ\text{C/min}$  under nitrogen flow ( $100 \text{ mL/min}$ ). The analysis software was used to precisely determine the decomposition temperature, termed the onset temperature ( $T_{\text{onset}}$ ).

#### 2.2.2. Characterization of the detonation products

The X-ray powder diffraction pattern of the detonation product was recorded on a D8Advance diffractometer using  $\text{Cu-K}\alpha$  radiation ( $\lambda = 1.54056 \text{ \AA}$ ) equipped with a Lynxeye detector and operating at 40 kV and 40 mA (Bruker, Billerica, MA, USA). The diffractogram was recorded from  $20$  to  $80^\circ$  with a  $2\theta$  step size of  $0.02^\circ$ . The microstructure of the sample was observed by scanning electron microscopy (SEM) on a DSM 982 Gemini (Zeiss) with a 10 kV current. The transmission electron microscopy (TEM) and high-resolution (HRTEM) images were collected by means of a JEM 2100F (JEOL, Tokyo, Japan) microscope operated at 200 kV. The diffraction patterns of the investigated material were recorded using the selected area electron diffraction mode with a 150 nm aperture or by Fourier transform of the HRTEM images. The specific surface area ( $a_s$ ) of the powder was determined by a nitrogen physisorption measurement carried out on a SA 3100 surface area analyser (Beckman Coulter, Brea, CA, USA). Prior to the measurement, the material was outgassed at 423 K for 10 h under a helium flow. The specific surface area was determined according to the Brunauer–Emmet–Teller (BET) method in the 0.05–0.20 relative pressure domain. The particle-size distributions of the different powders were established by the dynamic light scattering method using a Zetasizer nanoZS apparatus (Malvern Instrument, Worcestershire, United Kingdom). For that, a dispersion of the sample in ethanol solvent ( $0.1 \text{ g/L}$ ) was prepared.

## 3. Results and discussion

### 3.1. Characterization of the Emulstar 3000/ceramic precursor explosive emulsion

The sensitivity thresholds of the impact and friction tests tied to the onset temperature of decomposition of the zirconium-based energetic formulation are gathered in Table 2. For comparison, the values of the pure Emulstar 3000 explosive emulsion and standards required for ranking an energetic material as insensitive are also given [22,23]. As can be seen, both explosive emulsions (raw and mixed with a Zr-based salt) show total insensitivities to mechanical and thermal tests since their threshold values are higher than those mentioned by the standards

**Table 1**  
Characteristics of the Emulstar 3000 explosive emulsion.

Density ( $\text{g/cm}^3$ )	1.2–1.3
Detonation pressure (GPa) <sup>a</sup>	8
Detonation velocity (m/s.)	5000
Produced gas volume ( $\text{L/g}$ ) <sup>a</sup>	0.9
Oxygen balance ( $\text{g/100 g}$ ) <sup>a</sup>	−0.3
Energy ( $\text{cal/g}$ ) <sup>a</sup>	907

<sup>a</sup> Manufacturer's calculated parameters (Titanobel®).

**Table 2**

Sensitivity thresholds of the Emulstar 3000.

Sensitivity test	Impact (J)	Friction (N)	T <sub>onset</sub> (°C)
Standards (insensitivity)	>40	>360	>100
Emulstar 3000	>1200 <sup>a</sup>	>360 <sup>a</sup>	207.8
Emulstar 3000/Zr(SO <sub>4</sub> ) <sub>2</sub> ·4H <sub>2</sub> O	>49	>360	184.5

<sup>a</sup> Manufacturer's data and the Emulstar 3000/ceramic precursor mixture (90/10 wt %). The standards for an energetic material to be ranked as insensitive were added for comparison.

(>40 J, > 360 N and >100 °C for the impact, friction and thermal tests, respectively). It should be noted that for the impact test, the value > 49 J is the highest value that can be determined from our fall-hammer apparatus. Then, by comparison with the Emulstar 3000 counterpart, the as-prepared Emulstar3000/Zr(SO<sub>4</sub>)<sub>2</sub>·4H<sub>2</sub>O mixture shows a slight sensitization to thermal heating with an onset temperature of 184.5 °C (vs. 207.8 °C), which may come from accelerated ammonium nitrate decomposition (main component of the explosive emulsion) upon contact with the metal ion (zirconium); however, this does not prevent the preparation of the mixture and detonation experiments [24].

Finally, compared to the literature, the sensitivity thresholds of the as-formulated Emulstar3000/Zr(SO<sub>4</sub>)<sub>2</sub>·4H<sub>2</sub>O explosive emulsion, in particular the mechanical ones, are higher than those of the 1,3,5-trinitro-1,3,5-triazinane organic explosive (RDX, C<sub>3</sub>N<sub>3</sub>H<sub>6</sub>(NO<sub>2</sub>)<sub>3</sub>) used by A. A. Bukaemskii for the synthesis of zirconia nanoparticles [17]. In fact, the literature related threshold values are 7.5 J and 120 N for the RDX substance regarding the impact and friction tests, respectively [22,23]. Definitely, the explosive used in this work ensures total safety for the operator.

### 3.2. Characterization of the detonation product

Fig. 1 shows the X-ray diffraction pattern of the product obtained after the detonation of the Emulstar 3000/Zr(SO<sub>4</sub>)<sub>2</sub>·4H<sub>2</sub>O explosive charge and the purification steps. The most intense diffraction peaks were attributed to a tetragonal structure with the P4<sub>2</sub>/nmc space group describing the zirconium (IV) oxide structure (ZrO<sub>2</sub>, JCPDS card No. 72-7115). Miller planes were mentioned on the diffractogram. Other low intensity diffraction peaks observed on all the diffraction domains were assigned to a polymorph of the zirconia phase, namely, the monoclinic phase (P2<sub>1</sub>/c space group, JCPDS card No. 37-1484). For clarity's sake,

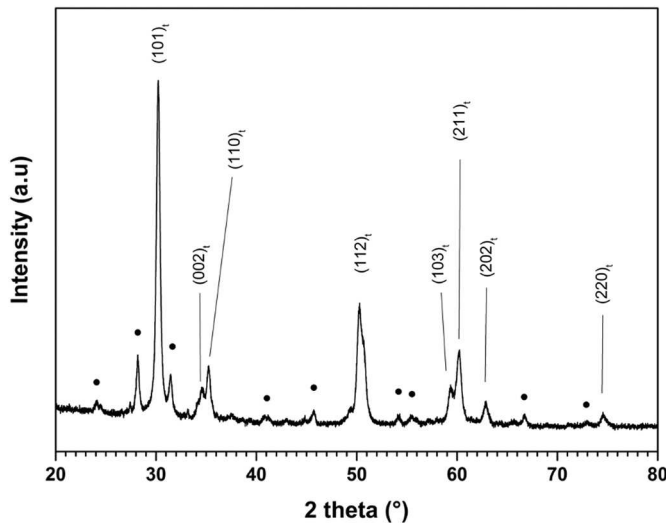


Fig. 1. XRD pattern of the zirconium (IV) oxide sample (ZrO<sub>2</sub>) synthesized by means of a zirconium-doped ammonium nitrate-based explosive emulsion detonation. The symbols t and ● are attributed to the tetragonal and monoclinic structures, respectively.

the corresponding Miller planes were not mentioned on the diffractogram. The volume fraction of the monoclinic phase ( $V_m$ ) in the ZrO<sub>2</sub> zirconia powder was determined by using the following formula (1) [25]:

$$V_m = \frac{1.311 \cdot X_m}{1 + 0.311 \cdot X_m} \quad (1)$$

where  $X_m$  corresponds to the integrated intensity ratio defined by formula (2):

$$X_m = \frac{I_{m(-111)} + I_{m(111)}}{I_{m(-111)} + I_{m(111)} + I_{t(101)}} \quad (2)$$

with  $I_{(hkl)}$  referring to the X-ray intensities of the diffraction peaks of the monoclinic and tetragonal phases identified by the subscripts m and t, respectively. The (-111) and (111) diffraction peaks characteristic of the monoclinic polymorph were located on both sides of the (101) most intense peak of the tetragonal structure (2 theta # 30°). A volume fraction of ~28% monoclinic phase was then calculated. The crystallite size or coherence length (D) of the ZrO<sub>2</sub> zirconia powder was determined from Scherrer's equation shown below (3):

$$D_{(hkl)} = \frac{K \cdot \lambda}{\beta \cdot \cos \theta} \quad (3)$$

where K is a dimensionless constant,  $\lambda$  is the X-ray wavelength of the radiation ( $\lambda = 1.54056 \text{ \AA}$  for copper radiation),  $\beta$  is the corrected peak width at half-maximum intensity and  $\theta$  is the diffraction peak position. Taking into account the most intense diffraction peak (101)<sub>t</sub>, the coherence length was estimated to be equal to 20.3 nm.

Fig. 2 shows TEM and HRTEM micrographs of the as-detonated zirconia powder. The zirconia powder can be described as being made of spherical particles, in which the particle-size distribution seems to be narrow and centred at approximately 20 nm, as depicted in Fig. 2A. The selected area electron diffraction pattern (SAED) exhibits diffraction rings with d spacings that could be attributed to the (101), (110) and (112) Miller planes, well-fitting to the P4<sub>2</sub>/nmc space group corresponding to the ZrO<sub>2</sub> tetragonal phase. The HRTEM images (Fig. 2B and C) show diffraction planes on numerous particles, thus confirming the high degree of crystallinity of the ZrO<sub>2</sub> powder synthesized by the detonation process. Moreover, the Fast Fourier transform done on HRTEM image of one nanoparticle (black square on Fig. 2C) permits to identify the (101) plane characteristic of tetragonal ZrO<sub>2</sub>. Fig. 3 shows representative SEM views of the as-detonated zirconium (IV) oxide powder. The low magnification pictures (Fig. 3A) present a powder made of agglomerated particles with the size of the primary particles strictly below the sub-micrometre range (<100 nm). The magnified SEM image, as shown in Fig. 3B, reveals a quasi-spherical morphology for the particles constituting the sample since the shape-factor seems to be very close to one. From the highest magnification view of the powder (Fig. 3C), the primary particle size can be estimated to be near 20-25 nm with a narrow particle size distribution. From a nitrogen physisorption measurement, the specific surface area of the as-detonated zirconium (IV) oxide powder was determined to be equal to 53 m<sup>2</sup>/g. This result is slightly higher than the one obtained by Ref. [19] (i.e., 35 m<sup>2</sup>/g). Assuming that the powder is made of monodispersed spherical and dense particles; the following formula (4) can be used to calculate the average diameter ( $\phi$ ) of the particles:

$$\phi = \frac{6}{\rho \times S_{BET}} \quad (4)$$

where  $\rho$  is the density of the material (5890 kg/m<sup>3</sup>) and  $S_{BET}$  is the specific surface area of the considered material. An average diameter of 19 nm was thus determined for the ZrO<sub>2</sub> particles.

By correlating the set of results obtained from the different characterization techniques (XRD, TEM and SEM), a monocrystalline character



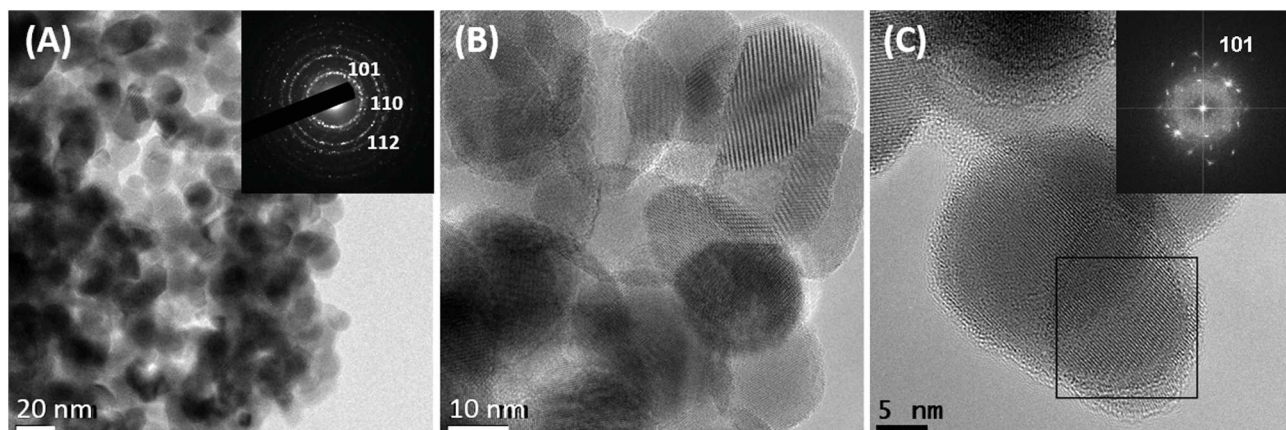


**Fig. 2.** TEM images of the  $\text{ZrO}_2$  powder synthesized by means of a zirconium-doped ammonium nitrate-based explosive emulsion detonation. a) Bright field TEM image combined with the SAED pattern using a aperture of 150 nm b) and c) HRTEM images showing the high cristallinity of the nanograins specially on c) with the FFT of the HRTEM image corresponding to the (101) planes of  $\text{ZrO}_2$  tetragonal.

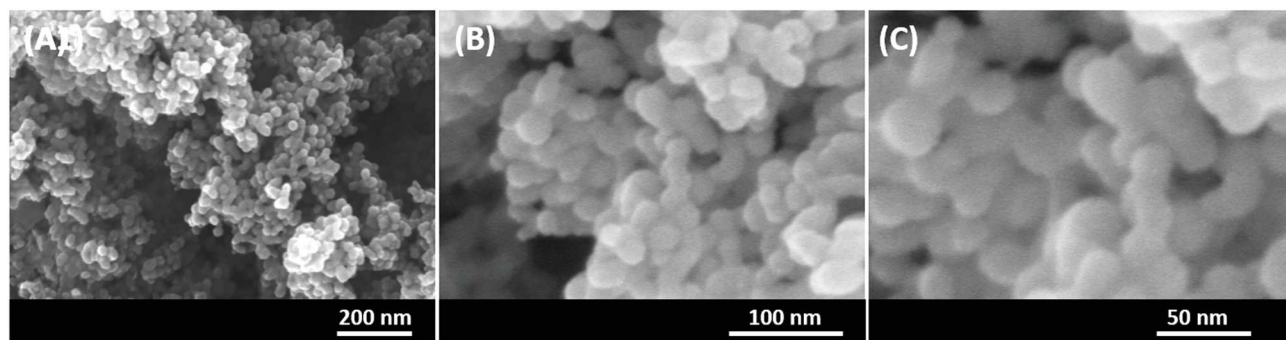


**Fig. 3.** SEM images in secondary electron mode of the  $\text{ZrO}_2$  powder synthesized by means of a zirconium-doped ammonium nitrate-based explosive emulsion detonation a) global view b) and c) same view with higher magnification.

of  $\text{ZrO}_2$  is expected.

Further characterization of the as-detonated  $\text{ZrO}_2$  powder was performed by dynamic light scattering diffusion. Fig. 4 gives the granulometric distribution both in terms of the volume and cumulative distributions as a function of the particle size. The volume distribution curve shows an aggregated powder with a size centred at 140 nm. From the cumulative volume distribution curve, cumulative volume

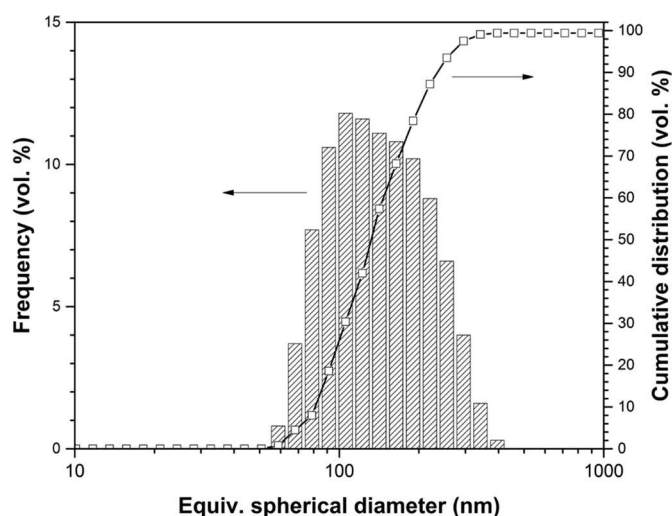


**Fig. 4.** Granulometric distributions of the  $\text{ZrO}_2$  powders synthesized by means of a zirconium-doped ammonium nitrate-based explosive emulsion detonation.

distributions ( $d_x$ ) were deduced, where  $d$  corresponds to the diameter of the particles or aggregates (in nm) and  $x$  is the volume percent. Approximate values of 90, 140, and 255 nm were found for the  $d_{10}$ ,  $d_{50}$  and  $d_{90}$  of the as-synthesized  $\text{ZrO}_2$ .

A way to evaluate the agglomeration state of the investigated powder is formula (5) described below and suggested by J. M. Haussonne et al. [3]:

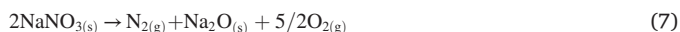
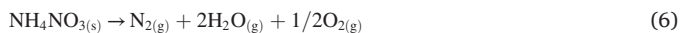
$$F_{AG} = d_{V50}/d_{BET} \quad (5)$$

where  $F_{AG}$  is the agglomeration factor,  $d_{V50}$  is the medium diameter in volume and  $d_{BET}$  is the average diameter deduced from the specific surface area of the considered powder. In the present case, a value of 7.5 was calculated for the zirconia powder, implying the dispersability of the as-detonated particles in liquid medium. To achieve a better possible dispersion, the experimental procedure will have to be improved.

A possible mechanism occurring during the detonation reaction of the mixture considered in the present work leading to the  $\text{ZrO}_2$  zirconia nanopowder synthesis can be suggested from the chemistry of explosives [26]. The composition of the ammonium nitrate-explosive is known to be 90 wt % (70 wt % ammonium nitrate ( $\text{NH}_4\text{NO}_3$ ) and 20 wt % sodium nitrate ( $\text{NaNO}_3$ )), with the rest consisting of water, oil and surfactant of an unknown chemical nature. To simplify the system, only the two nitrate salts will be taken into consideration as explosive sources, and the Zr-reactant will be regarded as an inert molecule.

The chemical reaction occurring when energetic molecules undergo an explosion can be described taking into account the amount of oxygen available during the reaction and provided by the reactants. These data are referenced as the oxygen balance (OB) [26]. Due to the OB value

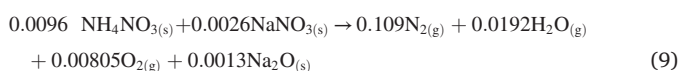
being positive, nil or negative, the molecule then contains an excess, sufficient or a default in the concentration of oxygen compared to that needed for complete oxidation. In the last case, toxic gases such carbon (CO) and nitrogen (NO) monoxides can be released. In the present work, the OB for ammonium nitrate and sodium nitrate are positive and are 19.99% and 45%, respectively, leading to the following decomposition chemical equations:



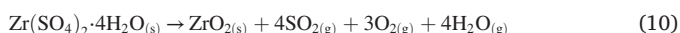
Now, considering an intimate mixture of both, the OB value ( $\text{OB}_{\text{AN/SN}}$ ) was calculated from equation (8):

$$\text{OB}_{\text{AN/SN}} = \text{OB}_{\text{AN}} \cdot C_{\text{AN}} + (1 - C_{\text{AN}}) \cdot \text{OB}_{\text{SN}} \quad (8)$$

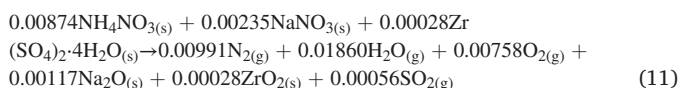
with OB and C being the oxygen balance and weight percent of each ingredient, respectively. Subscripts AN and SN are used for the ammonium and sodium nitrate compounds, respectively. The  $\text{OB}_{\text{AN/SN}}$  is 25.3%. The decomposition reaction can be thus rewritten, taking into the hypothesis 1 g of energetic composition (77.77 and 22.22 wt % of  $\text{NH}_4\text{NO}_3$  and  $\text{NaNO}_3$ , respectively) as follows:



Regarding the zirconium-ceramic salt, an inert molecule from a pyrotechnics point of view, the decomposition reaction can be defined as follows:



Now considering the three ingredients  $\text{NH}_4\text{NO}_3$ ,  $\text{NaNO}_3$  and  $\text{Zr}(\text{SO}_4)_2 \cdot 4\text{H}_2\text{O}$  and their respective weight amounts within the final explosive mixture (explosive emulsion/Zr-salt: 90/10 wt %), namely, 70, 20 and 10 wt %, respectively, the global detonation reaction of 1 g of mixture can be summarized by equation (11):



As the explosive charge is placed in a bag containing demineralized water, the  $\text{Na}_2\text{O}$  sodium oxide solid phase is converted into sodium hydroxide (NaOH) liquid phase during detonation. The zirconia solid material is the only solid phase formed during the detonation of the charge.

#### 4. Conclusion

A zirconium (IV) oxide powder was successfully synthesized via a detonation process implementing an insensitive ammonium-based explosive emulsion and a zirconium sulfate salt as the detonating substance and ceramic precursor, respectively. With an explosive substance/ceramic precursor weight ratio of 90/10, a nanosized  $\text{ZrO}_2$  powder was obtained. The resulting powder was composed of agglomerated spherical particles with an average diameter of 20 nm. Generally, the synthetic method executed here presents a simple, efficient and tuneable route, which is exploitable for producing ultra-fine oxide ceramic particles.

#### Credit author statement

**P. Gibot:** Conceptualization, Methodology, Investigation, Visualization, Writing-Original Draft. **F. Quesnay:** Investigation (Samples preparation). **C. Nicollet:** Investigation (Particles size analysis). **L. Laffont:** Investigation (HRTEM analysis). **F. Schnell:** Investigation (SEM analysis). **J. Mory:** Methodology, Investigation (Thermal

analysis). **D. Spitzer:** Supervision.

#### Declaration of competing interest

The authors declare that they have no known competing financial interests or personal relationships that could have appeared to influence the work reported in this paper.

#### Acknowledgements

The authors gratefully acknowledge the French National Centre for Scientific Research (CNRS), French German Research Institute of Saint-Louis (ISL, Saint-Louis, France) and University of Strasbourg (UNISTRA, Strasbourg, France) for funding. The authors express their acknowledgements to E. Fousson (ISL, Saint-Louis) for his assistance in the detonation experiments.

#### Appendix A. Supplementary data

Supplementary data to this article can be found online at <https://doi.org/10.1016/j.solidstatesciences.2020.106405>.

#### References

- [1] R. Riedel, I.W. Chen, *Ceramics Science and Technology - Vol. 2 Materials and Properties*, Wiley-VCH Verlag GmbH-Co., Weinheim, Germany, 2010.
- [2] <https://www.ceramtec.com/>.
- [3] J.M. Haussonne, C. Carry, P. Bowen, J. Barton, *Céramiques et verres – Principes et techniques d'élaboration. Traité des matériaux*, first ed., Presses polytechniques et universitaires romandes, Lausanne, Switzerland, 2005.
- [4] S.E. Pratsinis, Flame aerosol synthesis of ceramic powders, *Prog. Energy Combust. Sci.* 24 (1998) 197–219.
- [5] E.A. Levashov, A.S. Mukasyan, A.S. Rogachev, D.V. Shtansky, Self-propagating high-temperature synthesis of advanced materials and coatings, *Int. Mater. Rev.* 62 (2017) 203–239.
- [6] R.H.G.A. Kiminami, Combustion synthesis of nanopowders ceramic powders, *KONA Powder Particle J.* 19 (2001) 156–165.
- [7] S. Cudzilo, A. Maranda, J. Nowaczewski, R. Trebinski, W.A. Trzcinski, Detonative synthesis of inorganic compounds, *J. Mater. Sci. Lett.* 9 (2000) 1997–2000.
- [8] Groupe de travail de pyrotechnie spatiale (GTPS), *Dictionnaire de pyrotechnie*, seventh ed., Association française de pyrotechnie (AF3P), 2016.
- [9] V.M. Titov, V.F. Anisichkin, Mal'kov I. Yu, 9th Symposium on Detonation, 1989, p. 407. Portland.
- [10] O. Vasylykiv, Y. Sakka, V.V. Skorokhod, Nano-blast of nano-size  $\text{CeO}_2\text{-Gd}_2\text{O}_3$  powders, *J. Am. Ceram. Soc.* 89 (2006) 1822–1826.
- [11] X.H. Wang, X.J. Li, H.H. Yan, L. Xue, Y.D. Qu, G.L. Sun, Nano- $\text{MnFe}_2\text{O}_4$  powder synthesis by detonation of emulsion explosive, *Appl. Phys. A* 90 (2008) 417–422.
- [12] X. Xie, X. Li, Z. Zhao, H. Wu, Y. Qu, W. Huang, Growth and morphology of nanometer  $\text{LiMn}_2\text{O}_4$  powder, *Powder Technol.* 169 (2006) 143–146.
- [13] X. Li, Y. Qu, X. Xie, Z. Wang, R. Li, Preparation of  $\text{Sr}_2\text{Al}_2\text{O}_4\text{:Eu}^{2+}$ ,  $\text{Dy}^{3+}$  nanometer phosphors by detonation method, *Mater. Lett.* 60 (2006) 3673–3677.
- [14] Y. Qu, X. Li, X. Wang, D. Liu, Detonation synthesis of nanosized titanium oxide powders, *Nanotechnology* 18 (2007) 205602–205607.
- [15] X. Xie, X. Li, H. Yan, Detonation synthesis of zinc oxide nanometer powders, *Mater. Lett.* 60 (2006) 3149–3152.
- [16] A.A. Bukaemskii, Nanosize powder of zirconia. Explosive method of production and properties, *Combust. Explos. Shock Waves* 37 (2001) 481–485.
- [17] Zh.-W. Han, S. Xu, L.-F. Xie, Yu.-Ch. Han, Study on the application of emulsion explosives in synthesizing nanostructured ceria, *Combust. Explos. Shock Waves* 50 (2014) 477–482.
- [18] C. Da Silva, J. Manuel, A. Dos Santos, E. Marisa, Nanometric-sized ceramic materials, process for their synthesis and uses thereof 8 (557) (2013) 215. United States Patent.
- [19] Dos Santos A., Marisa E., Da Silva C., Manuel J., Lagoa C., Cia A.L., Process for nanomaterial synthesis from the preparation and detonation of an emulsion, products and emulsions thereof. United States Patent 9,115,001. 2015..
- [20] <http://www.innovnano.pt/>.
- [21] M.J. Langenderfer, W.G. Fahrenholtz, S. Chertopalov, Y. Zhou, V.N. Mochalin, C. E. Johnson, Detonation synthesis of silicon carbide nanoparticles, *Ceram. Int.* 46 (2020) 6951–6954.
- [22] NATO Standardization agreement, Explosives, Impact sensitivity tests, first ed., STANAG n°, 1999, p. 4489.
- [23] NATO Standardization agreement, Explosives, Friction sensitivity tests, first ed., STANAG n°, 2002, p. 4487.
- [24] NATO Standardization agreement, Explosives, thermal analysis using differential thermal analysis (DTA), differential scanning calorimetry (DSC), heat flow

- calorimetry (HFC), and thermogravimetric analysis (TGA), first ed., STANAG n°, 2002, p. 4515.
- [25] H.K. Schmidt, Quantitative analysis of polymorphic mixes of zirconia by X-ray diffraction, *J. Am. Ceram. Soc.* 70 (1987) 367–376.
- [26] J. Akhavan, *The Chemistry of Explosives*, second ed., The Royal Society of Chemistry, Cambridge, United Kingdom, 2014.